COMPUTER ANIMATION AND VIRTUAL WORLDS
Comp. Anim. Virtual Worlds 2008; **19**: 433–444
Published online 6 August 2008 in Wiley InterScience
(www.interscience.wiley.com) DOI: 10.1002/cav.235

Dynamic skin deformation with characteristic curves

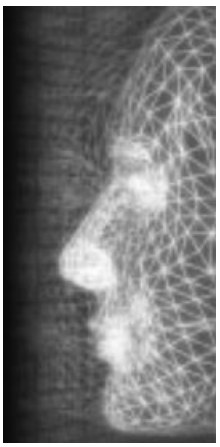

*By L. H. You, Xiaosong Yang and Jian J. Zhang**

By simulating motion and deformation of a set of 3D characteristic curves defining surfaces, we introduce a new skin deformation technique to animate skin deformation of character models. This technique consists of two parts, representation of characteristic curves and dynamic skin deformation. The first part is to extract characteristic curves of an existing model, that is a polygon model or a NURBS model, represent the characteristic curves with time-dependent 3D trigonometric curves, and relate the surface points of the model to these trigonometric curves. The advantage of such a treatment is that it can transform an original 3D problem into a 2D problem, making it much quicker and easier to process and compute. In the second part, a vector-valued dynamic fourth-order differential equation is employed to govern the behaviour of the time-dependent 3D trigonometric curves. These dynamic differential equations incorporate both the time component and the physical properties of the material, which are given by the user. Thus, the character model can be made to animate (deform) following the user-specified behaviour parameters. Our experiments demonstrate that this technique is able to produce realistic skin deformations efficiently and avoid the undesirable skinning problems suffered by some existing skinning techniques.

Received: 18 June 2008; Accepted: 23 June 2008

KEY WORDS: dynamic skin deformation; time-dependent 3D trigonometric curve; character animation

Introduction

Skin deformation is one of the most interesting and challenging topics in computer animation. Existing skin deformation methods can be classified into three categories: joint related, example based and physics based.

Joint-related methods deform the skin surface by a weighted combination of the joint transformations of the character's skeleton. One example in this category is the skeleton subspace deformation (SSD) which is also called linear blend skinning (LBS), vertex blending, enveloping or simple skinning. SSD is very fast and easy to use, and has been incorporated into many commercial animation software products. However, because it considers neither physical properties nor the underlying anatomical structures, the quality of animation depends almost exclusively on the judgment of the animator. It also suffers from some undesirable skin deformation artifacts such as the so-called collapsing joint and candy-wrapper effect. In addition, how to determine the blending weights requires skilled operations and it remains an open issue although some improvements have been made in recent years.

The example-based approaches treat skin deformation as an interpolation problem. Example skin models with different shapes in different poses from scanned data or sculpted models are interpolated with suitably chosen functions. This method can capture designed shapes including effects like muscle bulges and major wrinkles and generate high quality skinning from sample poses. However, they require sufficient example skin models to be produced.

Physics-based approaches are based on the anatomy, elastic mechanics or biomechanics of skin deformation originating from the movements of muscles and tendons. They are physically meaningful and have a

*Correspondence to: J. J. Zhang, The Media School, Bournemouth University, UK. E-mail: jzhang@bournemouth.ac.uk

capacity to generate more realistic simulation. Since muscles are made of nonlinear, approximately incompressible, anisotropic and hyperelastic materials, the exiting physical laws cannot describe complicated muscle deformations accurately and the feedback of animators during skeletal keyframing still represents a key element for animation production. In addition, physics-based approaches usually use numerical calculations which require specially trained users and often incur heavy computation expenses. Due to these reasons, physics-based skinning has not become popular in commercial animation.

In order to tackle the above problems, we propose a new skin deformation technique in this paper.

Any surface can be well defined by a curve network. When a surface physically deforms from a shape to another different shape, the curves defining the surface also change their shapes, caused by the forces acting on these curves. Based on this principle, the physical deformation of surfaces can be transformed into that of the curves which define the surfaces. This involves much fewer unknowns to be solved and has therefore higher computation efficiency compared with the direct surface-based approach. One can easily introduce necessary physical laws into the representation, leading to better realism of skin deformations than a purely geometric approach. In addition, feedback of animators can be easily introduced into the simulations.

Our proposed approach is motivated by the example- and physics-based methods. However, it is not the same as either. Our technique is supported by two theoretical elements: the representation of surface models with time-dependent 3D trigonometric curves and dynamic skin deformation based on the trigonometric curves. Our contributions are as follows:

1. Simplification of a surface model into a curve network by using characteristic curves to define the surface model and time-dependent 3D trigonometric curves to represent characteristic curves. It has three noticeable advantages. Unlike the traditional curves, the time-dependent 3D trigonometric curves can effectively represent a family of curves in a general equation with time t as its parameter. This is particularly beneficial to represent a deformation sequence. Unlike the existing cross-sectional contours, which are planar curves and ineffective in defining complex 3D surface shapes, our time-dependent 3D trigonometric curves are spatial and powerful in representing an arbitrary 3D shape. Compared to the cross-sectional ellipses, our method can approximate a given 3D model more accurately and create more realistic skin deformations.
2. Reduction of computing costs for the representation of character models. A character model, whether it is a polygon model or NURBS model, can be accurately defined using our technique with a lightweight representation. Since any 3D surface models involves two parametric variables and one time variable, and 3D curves only involves one parametric variable and one time variable, our approach transforms a 3D surface problem into a 2D curve problem. Since only a small amount of data is required to solve the linear equations, curve deformations are easy and fast to determine and skin deformation is achieved efficiently.
3. Creation of more realistic skin deformations through the introduction of physical properties. We employ dynamic fourth-order differential equations, which incorporate physical properties governing the dynamic behaviour of the skin of a character. In addition, the forces involved in the dynamic fourth-order differential equations also provide the animator with an effective editing tool for the animation of character skin shapes.

Related Work

Pioneering work of joint-related skin deformation was presented by Thalmann *et al.*[1] It was extended in References 2–8.

Example-based skin deformation was investigated by a number of researchers. These research studies include: pose space deformation (PSD),[9] weighted pose-space deformation (WPSD),[10] building character skins from examples,[6] example-based skin deformations,[11] example-based human hand model[12] and skeletal shape deformation based on given deformation examples.[13]

Physics-based approaches also attract a lot of research attention. Some work on skin deformations based on anatomy, elastic mechanics or biomechanics can be found in References 14–33.

Most character parts have a cylinder-like topology which can be represented with cross-sectional curves. This method has been investigated in References [34,35].

For complicated character models, 3D curves are more suitable. Such 3D curves have been employed to define surface models in existing References 36–38.

Recently, Au *et al.* used handle-aware isolines over deformation surfaces to build a reduced model and achieved detail-preserving deformation with resolution-

DOI: 10.1002/cav

independent periteration cost, fast convergence rate and linear memory cost.[39]

The cross-sectional contours are 2D time-independent geometric entities. They are applicable in defining static surface models. However, for the animation of skin deformations, 3D time-dependent curves would be a more suitable candidate, which will be presented later in this paper.

Since dynamic differential equations can help produce more realistic appearances and consequently reduce the amount of required example data, we will develop such a technique for dynamic skin deformations. First, the characteristic curves of a surface model are extracted and represented by time-dependent 3D trigonometric curves. How surface points of a model are related to these trigonometric curves is discussed. Then we introduce a dynamic skin deformation technique. Finally, we demonstrate the applications of our approach in the animation of skin deformations of virtual characters.

Time-Dependent 3D Trigonometric Curves

In this section, we discuss extraction and representation of 3D characteristic curves. Since NURBS models can be easily converted into polygon models, in the following, we only discuss how to treat polygon models.

Extraction of 3D Characteristic Curves

Using cross-section contours to represent surface models could be tricky, as the vertices of a model are not usually on the same planes. In addition, 2D curves are less flexible in describing complex surface shapes than their 3D counterparts. Due to these reasons, our first step is to extract 3D characteristic curves. Firstly, we separate a character model into different parts. As demonstrated in Figure 1a, a horse model is separated into ears, head, neck, torso, tail, fore legs and rear legs which are indicated with different colours. Then we subdivide each part of a character model into some regions according to distribution of surface points. For the horse model, we can further partition its parts into smaller regions as indicated by different colours shown in Figure 1b. The boundaries of each region are extracted and are called 3D characteristic curves. For the horse model, all extracted 3D characteristic curves are shown in Figure 1c.

In order to demonstrate different types of characteristic curves and the capability of our proposed dynamic skin deformation in treating complicated surface shapes, we use different methods to extract characteristic curves of the horse head and tail. When carrying out automatic extraction of characteristic curves, the same extraction method should be used. The existing segmentation approaches can be introduced to identify different parts.[40] According to shape changes of surface models, an automatic process can be used to generate a series of cross-sections which subdivide each part into smaller regions, and find out the surface points close to these cross-sections for the definition of characteristic curves.

When corresponding characteristic curves of a polygon model at different poses are to be extracted, the index of surface points on characteristic curves can be used to find out new positions of these surface points and determine new shapes of characteristic curves.

Representation of Time-Dependent 3D Trigonometric Curves

When a surface model moves or deforms, the characteristic curves on the model also change their positions

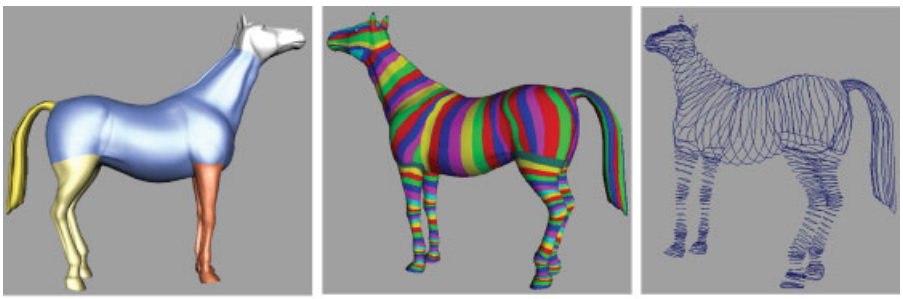

(a) (b) (c)

Figure 1. Extraction of 3D characteristic curves. (a) Model parts, (b) partitioned regions and (c) 3D characteristic curves.

DOI: 10.1002/cav

and shapes. Therefore, both the surface model and the corresponding characteristic curves are the functions of the time variable.

Since trigonometric series can describe complicated 3D curves with a single mathematical equation, we introduce a time variable into trigonometric series and develop the concept of time-dependent 3D trigonometric curves. Their mathematical form is a combination of the time variable t and trigonometric functions $\cos(2n\pi v)$ and $\sin(2n\pi v)$ $(n = 1, 2, \ldots, N)$, which are used to describe shapes of the characteristic curves and their motion and deformations.

$$q(v,t) = a_{q0} + \bar{a}_{q0}t + \bar{\bar{a}}_{q0}t^2 + \sum_{n=1}^{N}\left[(\bar{a}_{qn} + \bar{\bar{a}}_{qn}t)\right.$$
$$\left.\cos 2n\pi v + (\bar{b}_{qn} + \bar{\bar{b}}_{qn}t)\sin 2n\pi v\right] \; (q = x, y, z) \tag{1}$$

where x, y and z are the three coordinate values of a spatial point on the curves, v is a parametric variable, a_{q0}, $\bar{a}_{q0}$, $\bar{\bar{a}}_{q0}$, $\bar{a}_{qn}$, $\bar{\bar{a}}_{qn}$, $\bar{b}_{qn}$ and $\bar{\bar{b}}_{qn}$ $(n = 1, 2, 3, \cdots, N)$ are unknown constants and N is the total term of the trigonometric functions.

Although other forms of the time-dependent 3D curves may also be applicable, our investigation below suggests that dynamic skin deformations of virtual characters can be well described with Equation (1).

At any instant, the time variable t is a constant and Equation (1) for this instant becomes

$$q(v) = e_{q0} + \sum_{n=1}^{N}(e_{q2n-1}\cos 2n\pi v + e_{q2n}\sin 2n\pi v) \tag{2}$$

where e_{qm} $(m = 0, 1, 2, 3, \cdots, 2N)$ are unknowns.

When 3D characteristic curves are closed, the unknown constants in Equation (2) can be directly determined from the coordinate values of the vertices on the characteristic curves by curve fitting. When the 3D characteristic curves are open, we substitute the values of both end points of the characteristic curves into Equation (2) and use the in-between vertices on the characteristic curves for curve fitting and for determining the rest unknown constants.

Compared to the surface modelling with standard elliptic cross-sections, the advantages of our method include extending from 2D to 3D and from time independent to time dependent. In addition, our modelling method has a higher accuracy.

In Figure 2, we give some cross-section curves of the legs from a human model and their fitted elliptic curves. Those in red and blue are the original and elliptic cross-sections, respectively. It can be seen from these images

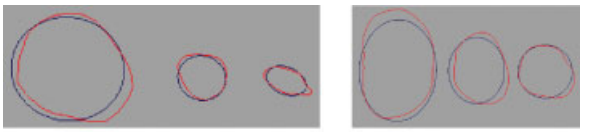

(a) (b)

Figure 2. Comparison between real human cross-sections and approximated ellipses. (a) From right leg and (b) from left leg.

that there are noticeable differences between the real cross sections and elliptic ones.

For the cross-sectional curves taken from a human leg and torso, we use our proposed time-dependent 3D trigonometric curves to regenerate them and the obtained results are given in Figure 3 where the curves in red, green and blue are the original ones, those produced using our approach and those created with the standard ellipses, respectively. It can be seen from the figures that our algorithm approximates cross-sectional curves of a surface model with excellent accuracy.

In Figure 4, we demonstrate the ability of our time-dependent trigonometric curves to fit arbitrary spatial curves. In this figure, the blue ones are the original 3D curves, and the red ones are produced by our algorithm. Our method offers an accurate approximation.

In Figure 5, three original curves on the left are consecutively changed into the final shape on the right. We use our time-dependent trigonometric curves (1) to describe the curve shapes of this deformation sequence.

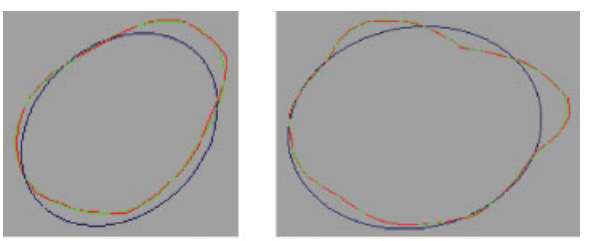

(a) (b)

Figure 3. Cross-sectional curve generation with different approaches. (a) From a leg and (b) from a torso.

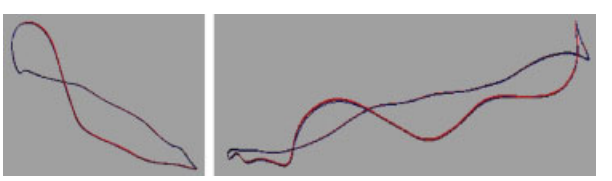

Figure 4. Spatial curve generation with time-dependent 3D trigonometric curves.

DOI: 10.1002/cav

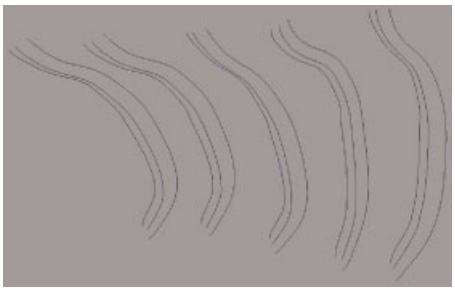

Figure 5. Representation of curve deformation sequence by time-dependent 3D trigonometric curves.

Between the initial and final shapes are the in-between ones generated with our algorithm. These images demonstrate the effectiveness of our approach in the description of a deformation sequence of 3D curves.

Relating Surface Points to Time-Dependent 3D Trigonometric Curves

We can rebuild a surface model from time-dependent 3D trigonometric curves, or relate surface points of a model to these curves. We will introduce the former in our another paper and the latter in this paper.

For point p on a trigonometric curve $q_i(v)$, its coordinate values can be determined by $q_i(v_p)$. For point p between two curves $q_i(v)$ and $q_{i+1}(v)$, we use the following subdivision algorithm to determine its position. First, we find four points 1, 2, 3 and 4 on $q_i(v)$ and $q_{i+1}(v)$ which are the closest to the pink point p and point p should fall within the quadrilateral formed by these four points as shown in Figure 6. Then we find points 5 and 7 by $q_i(v_5)$ and $q_{i+1}(v_7)$ where $v_5 = v_1 + (v_4 - v_1)/2$ and $v_7 = v_2 + (v_3 - v_2)/2$. Next, we obtain midpoint 9 between points 5 and 7, midpoint 8 between 3 and 4 and midpoint 6 between 1 and 2. The region 1–2–3–4 is divided into four small regions 1–6–9–5, 6–2–7–9, 9–7–3–8 and 5–9–8–4. The new region 5–9–8–4 where point p situates is subdivided into four smaller regions 5–12–14–11, 12–9–13–14, 14–13–8–10 and 11–14–10–4 with point p in region 5–12–14–11. This process is repeated until the region with point p is reduced to the required accuracy.

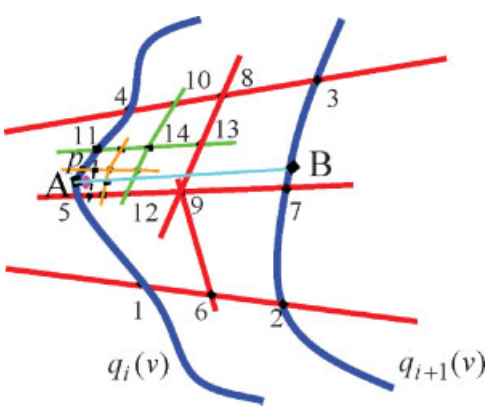

Figure 6. Determination of surface points.

For the pink point p, the above subdivision algorithm gives $v_A = v_1 + 9(v_4 - v_1)/16$, $v_B = v_2 + 9(v_3 - v_2)/16$, $q_i(v_A)$, $q_{i+1}(v_B)$ and $D_{Ap} = D_{AB}/32$ where D_{AB} is the distance between points A and B.

After curves $q_i(v)$ and $q_{i+1}(v)$ are deformed into $q_i'(v)$ and $q_{i+1}'(v)$, points A, p and B are moved to A', p' and B'. An interpolation surface is created from the deformed curves and the coordinate values of point p' on the interpolation surface are obtained from v_A, v_B, $q_i'(v_A)$, $q_{i+1}'(v_B)$ and $D_{A'p'} = D_{A'B'}/32$, which relate surface point p' to time-dependent 3D trigonometric curves.

Dynamic Skin Deformation

After transforming a surface model into trigonometric curves, the motion and deformation of the surface model are changed into those of the corresponding curves.

Mathematical Model

A curve can be regarded as a physical wire which has material properties such as Young's modulus, density ρ and damping coefficient η. Among them, Young's modulus contributes to static elastic deformations, and the density and damping coefficient are related to the motion and dynamic deformation of the wire. Subject to externally applied forces, such a wire will move and deform.

The dynamic deformations of a wire can be represented by vector-valued dynamic fourth-order differential equations. They are derived with the same methodology as the dynamic deformations of an elastic beam and have the form of

$$a_{1q}\frac{\partial^4 q(v,t)}{\partial v^4} + a_{2q}\frac{\partial^2 q(v,t)}{\partial v^2} + \rho\frac{\partial^2 q(v,t)}{\partial t^2} + \eta\frac{\partial q(v,t)}{\partial t} = F_q(v,t) \quad (3)$$

where a_{1q} and a_{2q} are shape control parameters which are related to static material properties and $F_q(v,t)$ is an externally applied force.

DOI: 10.1002/cav

The motion and deformations of a curve determined by this equation should present a more realistic description, due to the consideration of physical laws. The remaining work is how to solve this equation and employ the solution to represent motion and deformations of 3D curves.

Resolution

The dynamic fourth-order differential equation (3) can be applied in two different ways. If only the shape of a skin surface model at one pose is known, we can apply some forces on the time-dependent 3D trigonometric curves, and solve Equation (3) to obtain the deformation of the model. If the skin shapes are known at two different poses, we can use these skin shapes to determine forces at these two poses and their variation, and obtain all the skin shapes between the initial and final poses using Equation (3). For the former, the key to success is to determine a proper force distribution on the initial skin surface and the variation of these forces. Compared to the former, the latter requires one more skin shape but eliminates the preparation work in force application and manipulation. Here, we investigate the latter.

According to the mathematical description of our proposed time-dependent 3D trigonometric curves and dynamic fourth-order differential equation (3), the forces can have the following form

$$F_q(v,t) = \bar{c}_{q0}(1+t) + \sum_{n=1}^{N}\left[(\bar{c}_{qn} + \bar{\bar{c}}_{qn}t) \cos 2n\pi v + (\bar{d}_{qn} + \bar{\bar{d}}_{qn}t)\sin 2n\pi v\right] \tag{4}$$

Substituting Equations (1) and (4) into Equation (3), and inserting the obtained unknown constants into Equation (1), the mathematical representation of the time-dependent 3D trigonometric curves arrives, which represent the deformed skin at any poses

$$\begin{aligned} q(v,t) = {} & a_{q0} + \frac{t}{\eta}\bar{c}_{q0} + \frac{t}{\eta}(\frac{t}{2} - \frac{\rho}{\eta})\bar{c}_{q0} \\ & + \sum_{n=1}^{N}\left\{\frac{1}{A_n}\left[\bar{c}_{qn} + (t - \frac{\eta}{A_n})\bar{\bar{c}}_{qn}\right]\cos 2n\pi v \right. \\ & \left. + \frac{1}{A_n}\left[\bar{d}_{qn} + (t - \frac{\eta}{A_n})\bar{\bar{d}}_{qn}\right]\sin 2n\pi v\right\} \end{aligned} \tag{5}$$

where

$$A_n = 4\pi^2 n^2 (4\pi^2 n^2 a_{1q} - a_{2q}) \tag{6}$$

Through Equation (5), dynamic deformations q of time-dependent 3D trigonometric curves are related to the applied forces.

If the skin shapes at the initial pose $t = 0$ and the final pose $t = 1$ are known, we first extract characteristic curves (as discussed in Subsection 3.1) to define these two skin surfaces. Let us use subscript 0 to stand for the initial pose, subscript 1 for the final pose, I for the total number of the points at one characteristic curve and q_{i0} and $q_{i1} (q = x, y, z;\ i = 1, 2, 3, \cdots, I)$ to represent the points at a characteristic curve of these two skin surfaces. If there is a rigid motion from the initial pose to the final pose, we can use geometric transformation to remove it before the application of the dynamic differential equation (3).

Setting $t = 0$ in Equation (5) and making it have the same value as q_{i0} at point i, the following equations are produced

$$\begin{aligned} & a_{q0} + \sum_{n=1}^{N}\left[\frac{1}{A_n}\left(\bar{c}_{qn} - \frac{\eta}{A_n}\bar{\bar{c}}_{qn}\right)\cos 2n\pi v_i \right. \\ & \left. + \frac{1}{A_n}\left(\bar{d}_{qn} - \frac{\eta}{A_n}\bar{\bar{d}}_{qn}\right)\sin 2n\pi v_i\right] - q_{i0} = 0 \\ & (i = 1, 2, 3, \cdots, I) \end{aligned} \tag{7}$$

Similarly, substituting $t = 1$ into Equation (5) and making it have the same value as q_{i1} at point i, we obtain the below equations:

$$\begin{aligned} & a_{q0} + \frac{1}{\eta}\bar{c}_{q0} + \frac{1}{\eta}(\frac{1}{2} - \frac{\rho}{\eta})\bar{c}_{q0} \\ & + \sum_{n=1}^{N}\left\{\frac{1}{A_n}\left[\bar{c}_{qn} + (1 - \frac{\eta}{A_n})\bar{\bar{c}}_{qn}\right]\cos 2n\pi v_i \right. \\ & \left. + \frac{1}{A_n}\left[\bar{d}_{qn} + (1 - \frac{\eta}{A_n})\bar{\bar{d}}_{qn}\right]\sin 2n\pi v_i\right\} - q_{i1} = 0 \\ & (i = 1, 2, 3, \cdots, I) \end{aligned} \tag{8}$$

Taking $I \geq 2N + 1$ and solving Equations (7) and (8), we determine all the unknown constants in Equation (5).

Setting the time variable t to different values, different skin shapes at any poses between the initial and final poses are generated with the time-dependent 3D trigonometric curves presented by Equation (5).

If the skin shapes at two other poses $t = t_0 \neq 0$ and $t = t_1 \neq 1$ are known, we can still use the above method to determine the unknown constants in Equation (5) and create all skin surfaces between the initial and final poses.

DOI: 10.1002/cav

Editing In-Between Deformed Curves

Although the forces and skin deformations can be automatically determined with Equation (5), our proposed approach allows the manual editing of the time-dependent trigonometric curves to create more realistic deformation through the transformation of these curves and manipulation of the forces. After the modification of the characteristic curves, Equations (7) and (8) are solved within new resolution regions. For example, if we manually modify one middle deformed surface generated by Equation (5), we can solve Equations (7) and (8), respectively, using the initial surface and the modified middle surface, and the modified middle surface and the final surface. With this treatment, we can create skin deformations more suited to the user's taste.

Experimental Results

In this section, we present some examples to demonstrate applications of our proposed dynamic skin deformations based on time-dependent 3D trigonometric curves.

The first example is to animate a human arm and examine whether our method can avoid artefacts like collapsing joints. The surface shapes at the initial and final poses are shown in Figures 7a and 7j.

The upper arm is represented with nine characteristic curves. On each characteristic curve, 31 points are employed to solve Equations (7) and (8), and determine the time-dependent 3D trigonometric curves (5). The obtained initial and final surfaces from the curves (5) are the same as those in Figures 7a and 7j, indicating that the original surface has been well described with the trigonometric curves. The original polygon model of the upper arm has 1150 vertices and 1080 faces. With our representation, the total parameters used to determine all surface shapes of the upper arm from the initial pose to the final pose are 558, with a significant reduction of the data required. According to Gaussian elimination, the number of algebraic operations to solve linear equations of 1150×3 unknown constants is about 3450^3. Our method is to solve a series of small linear equations of 62 unknown constants. The number of algebraic

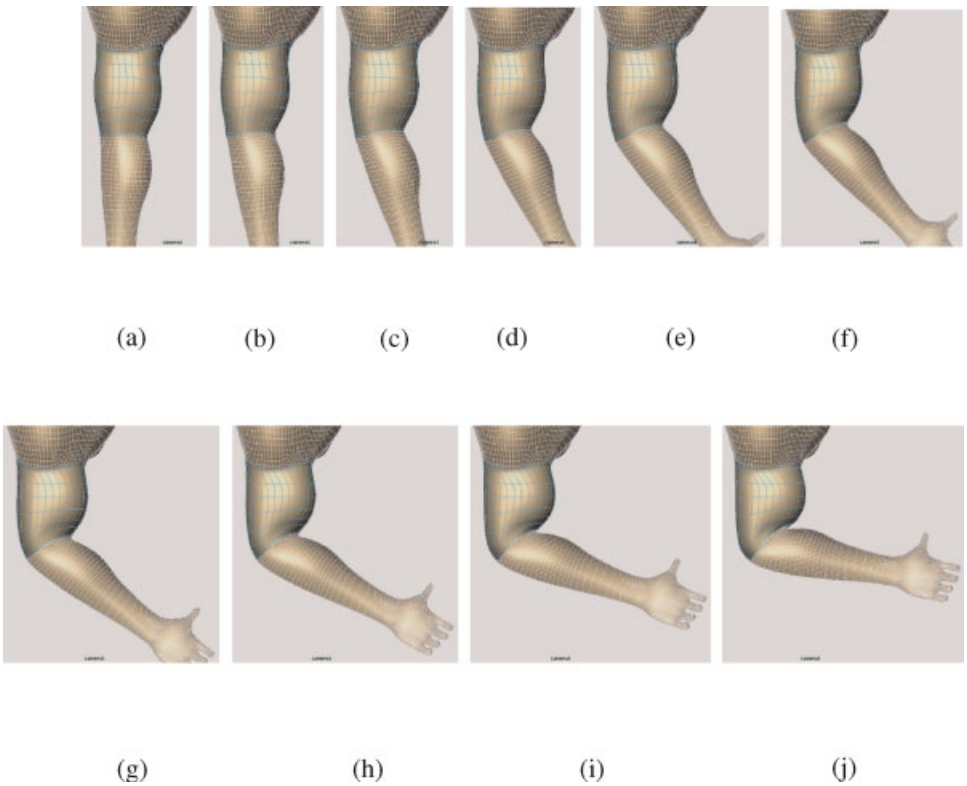

Figure 7. Human arm animation and skin deformations: (a) Initial known pose at $t = 0$, (b)–(i) indicate the calculated shapes at $t = i/9$, where $i = 1, 2, \ldots, 8$, (j) final known pose at $t = 1$.

DOI: 10.1002/cav

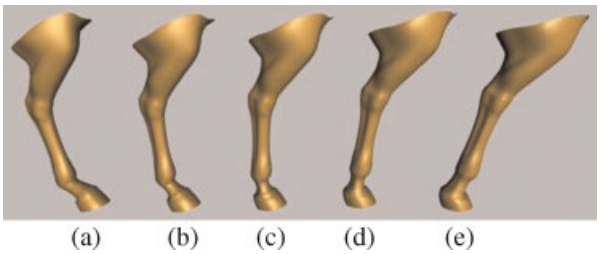

Figure 8. Horse leg animation and skin deformation: (a) initial known pose at $t=0$, (b) another known pose at $t=0.25$, (c) calculated shape at $t=0.5$, (d) calculated shape at $t=0.75$ and (e) calculated shape at $t=1$.

operations is $62^3 \times 3 \times 9$ which is 1/6381 of 3450^3. Therefore, it is fast enough for any form of animation product.

Setting the time variable to different values, we have created its animation. Figures 7b–7i give surface shapes at $t=i/9$ ($i=1, 2, 3, \ldots, 8$). No anomaly occurs in the resulting skin deformation.

The second example is to animate a horse leg. Different from the above example where the deformations at the initial and final poses are known, the known information for this example is an initial pose at $t=0$ shown in Figure 8a and another pose at $t=0.25$ as

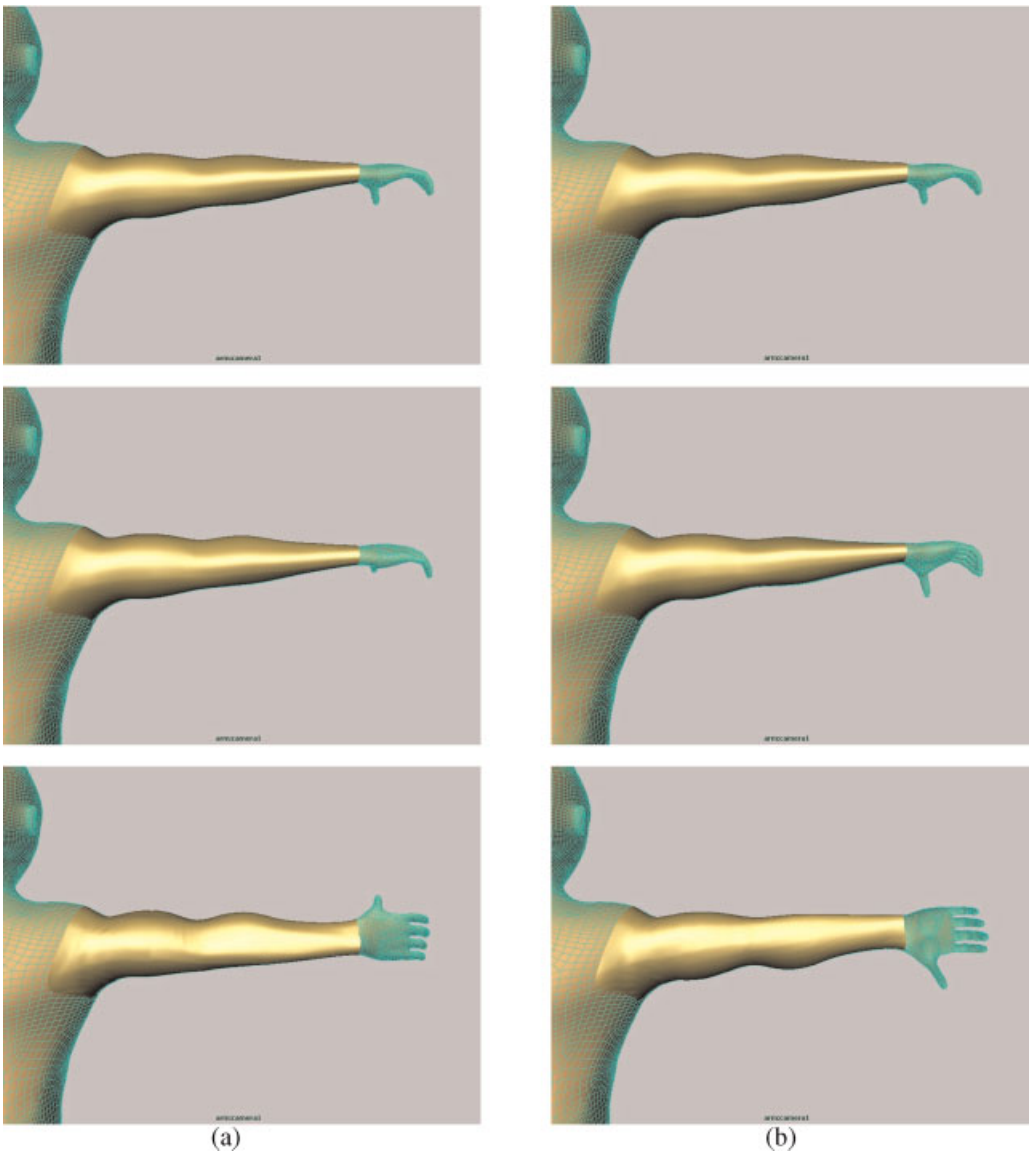

Figure 9. Twist deformations: (a) the arm is twisted upwards and (b) the arm is twisted downwards.

Comp. Anim. Virtual Worlds 2008; **19**: 433–444
DOI: 10.1002/cav

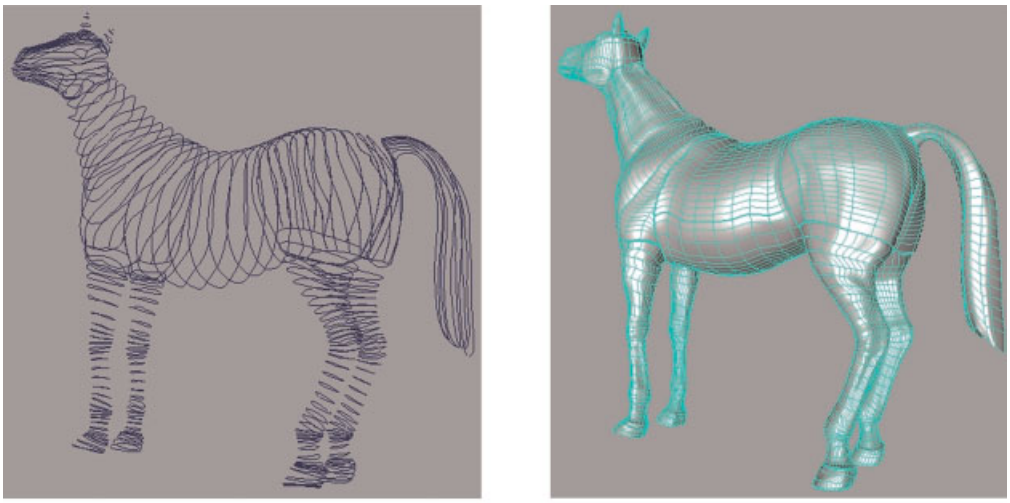

(a) (b)

Figure 10. Representation of a horse model: (a) network of time-dependent 3D trigonometric curves and (b) surface model defined by the network.

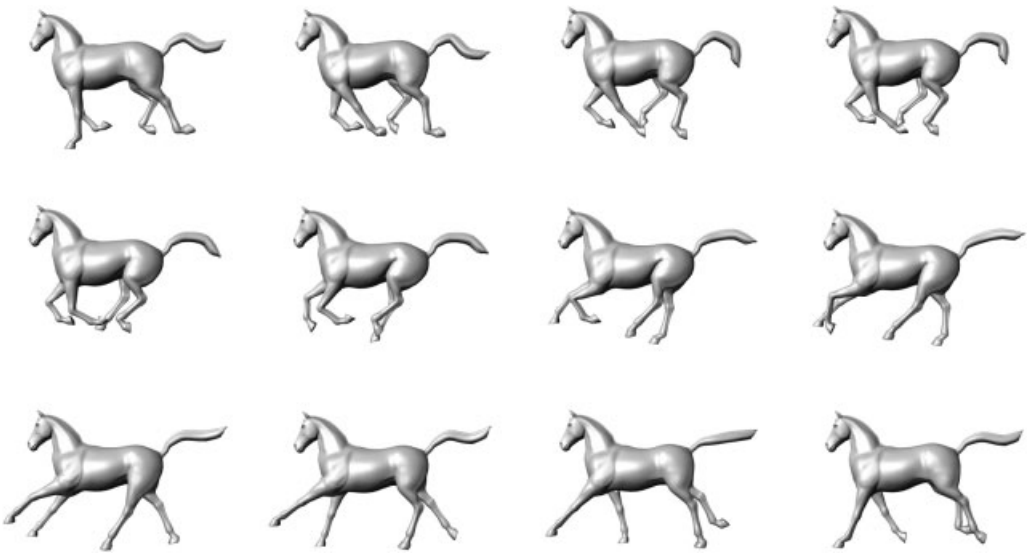

Figure 11. Horse animation and skin deformations.

shown in Figure 8b (the total deformation sequence is from $t=0$ to $t=1$). Setting $t=0$ and $t=0.25$ in Equation (5), respectively, and substituting the shape information of the horse leg at these poses into the equation, we determined all the unknown constants. Equation (5) is able to produce all the shapes between $t = 0$ and $t = 1$, giving plausible extrapolations. Figure 8 shows the snapshots of the horse leg model at $t=0.5$, $t=0.75$ and $t=1$.

In the third example, we twist a human arm model and examine whether the candy-wrapper anomaly arises. We build an original arm model shown in the top row of the images in Figure 9 and two adjacent twisted shapes which are twisted a little upwards and downwards, respectively, and are given in the middle row of the images in Figure 9. Using the same method as that for the horse leg example and setting the poses corresponding to the top and middle images to be at

DOI: 10.1002/cav

$t = 0$ to $t = 0.1$, we produce all the twisted deformations between $t = 0$ and $t = 1$. The images at the bottom row of Figure 9 are the twisted shapes at $t = 1$. No candy-wrapper collapse problems are produced with our dynamic shape deformation technique.

Our final example is to represent and animate a horse model. After partitioning the horse model, the characteristic curve representing the boundary of two adjacent regions is represented with a time-dependent 3D trigonometric curve. This results in a network of the trigonometric curves (Figure 10a). The horse model defined by these trigonometric curves is given in Figure 10b.

The original polygon horse model has 8431 vertices, 25 274 edges and 16 843 faces. With our approach, the total parameters used to define the whole horse model are 4340, which is much lighter than the original one.

The horse motion is divided into different stages. For each stage, we extract the skin shape information of the horse model at the initial and final poses. With the information, we solve Equations (7) and (8) to obtain the time-dependent 3D trigonometric curves and use them to create in-between shapes at different poses. Figure 11 shows some skin shapes of the horse model which are taken from the accompanying video.

Conclusions and Future Work

A dynamic skin deformation technique has been developed for realistic animation of virtual characters. This technique has two elements: representation of surface models with time-dependent 3D trigonometric curves and dynamic simulation of skin deformations. By extracting characteristic curves from an existing surface model (e.g. polygon or NURBS) and representing these characteristic curves with our time-dependent 3D trigonometric curves, the original model is transformed into a simpler network of curves which is used in the subsequent skin animation.

By introducing the dynamic fourth-order differential equations and forces, one can easily represent and manipulate the skin surfaces dynamically. We have developed a simple method to quickly create all skin shapes without introducing unwanted artefacts, unlike the LBS commonly used in the animation industry. The examples shown in this paper demonstrate the usefulness and capacity of our technique in the animation of character skin shapes dynamically.

Using deformations of time-dependent 3D trigonometric curves to define and animate a surface model is a new exploration. There are a number of issues requiring further investigations. These issues include intersection between time-dependent 3D trigonometric curves, simulation of skin vibration and skin wrinkles, and volume preservation, etc. Although these issues have not been discussed in this paper due to the limited space, they are easy to tackle. The intersection between trigonometric curves can be transformed into the intersection between the surface patches, which are defined by two adjacent trigonometric curves. Collision avoidance constraints can be used to prevent such intersections during animation. Skin vibration can be changed into vibration of the time-dependent 3D trigonometric curves defining the skin surface through the same dynamic equation. Skin wrinkles can be obtained by using the distance constraint between two adjacent trigonometric curves and volume preservation can be achieved by introducing a volume constraint into the deformation simulation. We intend to study these issues and implement necessary techniques in our future work.

ACKNOWLEDGEMENTS

We are grateful to Autodesk for their donation of the Maya software licenses. The mesh data used in this project was made available by Robert Sumner and Jovan Popović from the Computer Graphics Group at MIT. This research is in part supported by the Great Western Research Fellowship grant and EPSRC grant EP/F030355/1.

References

1. Thalmann NM, Laperrière R, Thalmann D. Joint-dependent local deformations for hand animation and object grasping. In *Proceedings of Graphics Interface*, 1988; 26–33.
2. Lander J. Skin them bones: game programming for the web generation. *Game Developer Magazine* May 1998; 11–16.
3. Lander J. Over my dead, polygonal body. *Game Developer Magazine* October 1999; 11–16.
4. Weber J. Run-time skin deformation. In *Proceedings of Game Developers Conference*, 2000.
5. Wang XC, Phillips C. Multi-weight enveloping: least-squares approximation techniques for skin animation. In *Proceedings of 2002 ACM SIGGRAPH/Eurographics Symposium on Computer Animation*, ACM Press, 2002; 129–138.

DOI: 10.1002/cav

6. Mohr A, Gleicher M. Building efficient, accurate character skins from examples. *ACM Transactions on Graphics (SIGGRAPH 03)* 2003; **22**(3): 562–568.
7. Kavan L, Žára J. Spherical blend skinning: a real-time deformation of articulated models. In *Proceedings of the 2005 Symposium on Interactive 3D Graphics and Games*, 2005; 9–16.
8. Yang XS, Somasekharan A, Zhang JJ. Curve skeleton skinning for human and creature characters. *Computer Animation and Virtual Worlds* 2006; **17**: 281–292.
9. Lewis LP, Cordner M, Fong N. Pose space deformation: a unified approach to shape interpolation and skeleton-driven deformation. In *Proceedings of the 27th Annual Conference on Computer Graphics and Interactive Techniques*, ACM Press/Addison-Wesley Publishing Co, 2000; 165–172.
10. Rhee T, Lewis JP, Neumann U. Real-time weighted pose-space deformation on the GPU. *Computer Graphics Forum* 2006; **25**(3): 439–448.
11. Allen B, Curless B, Popović Z. Articulated body deformation from range scan data. *ACM Transactions on Graphics (SIGGRAPH 02)* 2002; **21**(3): 612–619.
12. Kurihara T, Miyata N. Modeling deformable human hands from medical images. In *Proceedings of the 2004 ACM SIGGRAPH/Eurographics Symposium on Computer Animation*, Eurographics Association, 2004; 355–363.
13. Weber O, Sorkine O, Lipman Y, Gotsman C. Context-aware skeletal shape deformation. *Computer Graphics Forum* 2007; **26**(3): 265–274.
14. Chen DT, Zeltzer D. Pump it up: computer animation of a biomechanically based model of muscle using the finite element method. In *SIGGRAPH*, 1992; 89–98.
15. Scheepers F, Parent RE, Carlson WE, May SF. Anatomy-based modelling of the human musculature. In *Proceedings of the 24th Annual Conference on Computer Graphics and Interactive Techniques*, ACM Press/Addison-Wesley Publishing Co., 1997; 163–172.
16. Wilhelms J, Van Gelder A. Anatomically based modelling. In *Proceedings of the 1997 Conference on Computer Graphics*, ACM Press, 1997; 173–180.
17. Nedel LP, Thalmann D. Modeling and deformation of the human body using an anatomically-based approach. In *Proceedings of the Computer Animation*, IEEE Computer Society, 1998; 34–40.
18. Nedel L, Thalmann D. Anatomic modelling of deformable human bodies. *The Visual Computer* 2000; **16**(6): 306–321.
19. Aubel A, Thalmann D. Interactive modelling of the human musculature. In *Proceedings of the 14th Conference on Computer Animation*, Institute of Electrical and Electronics Engineers Inc., 2001; 167–173.
20. Simmons M, Wilhelms J, Van Gelder A. Model-based reconstruction for creature animation. In *Proceedings of the 2002 ACM SIGGRAPH/Eurographics Symposium on Computer Animation*, Institute of Electrical and Electronics Engineers Inc., 2002; 139–146.
21. Capell S, Green S, Curless B, Duchamp T, Popović Z. Interactive skeleton-driven dynamic deformations. *ACM Transactions on Graphics (SIGGRAPH 02)* 2002; **21**(3): 586–593.
22. James DL, Pai DK. DyRT: dynamic response textures for real time deformation simulation with graphics hardware. *ACM Transactions on Graphics (SIGGRAPH 02)* 2002; **21**(3): 582–585.
23. Larboulette C, Cani M-P. Real-time dynamic wrinkles. In *Proceedings of the Computer Graphics International (CGI'04)*, IEEE Computer Society Press, Washington, DC, USA, 2004; 522–525.
24. Guo Z, Wong KC. Skinning with deformable chunks. *Computer Graphics Forum* 2005; **24**(3): 373–381.
25. Venkataraman K, Lodha S, Raghavan R. A kinematic-variational model for animating skin with wrinkles. *Computers & Graphics* 2005; **29**(5): 756–770.
26. Larboulette C, Cani M-P, Arnaldi B. Dynamic skinning: adding real-time dynamic effects to an existing character animation. In *Proceedings of the 21st Spring Conference on Computer Graphics*, ACM Press, New York, NY, USA, 2005; 87–93.
27. Pratscher M, Coleman P, Laszlo J, Singh K. Outside-in anatomy based character rigging. In *Proceedings of 2005 ACM SIGGRAPH/Eurographics Symposium on Computer Animation*, ACM Press, New York, USA, 2005; 329–338.
28. Teran J, Sifakis E, Blemker SS, Ng-Thow-Hing V, Lau C, Fedkiw R. Creating and simulating skeletal muscle from the visible human data set. *IEEE Transactions on Visualization and Computer Graphics* 2005; **11**(3): 317–328.
29. Von Funck W, Theisel H, Seidel H-P. Vector field based shape deformations. *ACM Transactions on Graphics (SIGGRAPH 06)* 2006; **25**(3): 1118–1125.
30. Merry B, Marais P, Gain J. Animation space: a truly linear framework for character animation. *ACM Transactions on Graphics* 2006; **25**(4): 1400–1423.
31. Yang XS, Zhang JJ. Automatic muscle generation for character skin deformation. *Computer Animation and Virtual Worlds* 2006; **17**: 293–303.
32. Capell S, Burkhart M, Curless B, Duchamp T, Popović Z. Physically based rigging for deformable characters. *Graphical Models* 2007; **69**(1): 71–87.
33. Angelidis A, Singh K. Kinodynamic skinning using volume-preserving deformations. In *Proceedings of 2007 ACM SIGGRAPH/Eurographics Symposium on Computer Animation*, Eurographics Association Aire-la-Ville, Switzerland, 2007; 129–140.
34. Shen J, Thalmann NM, Thalmann D. Human skin deformation from cross sections. In *Proceedings of Computer Graphics International*, Melbourne, Australia, 1994.
35. Hyun D-E, Yoon S-H, Chang J-W, Seong J-K, Kim M-S, Jüttler B. Sweep-based human deformation. *The Visual Computer* 2005; **21**: 542–550.
36. Singh K, Fiume E. Wires: a geometric deformation technique. In *SIGGRAPH, 1998*; 405–414.
37. Pyun H, Shin HJ, Shin SY. On extracting the wire curves from multiple face models for facial animation. *Computers & Graphics* 2004; **28**(5): 757–765.
38. You LH, Yang XS, Pachulski M, Zhang JJ. Boundary constrained swept surfaces for modelling and animation. *Computer Graphics Forum* 2007; **26**(3): 313–322.
39. Au OKC, Fu H, Tai CL, Cohen-Or D. Handle-aware isolines for scalable shape editing. *ACM Transactions on Graphics (SIGGRAPH 07)* 2007; **26**(3): 83-1–83-10.
40. Shamir A. A survey on mesh segmentation techniques. *Computer Graphics Forum* 2008; 1–18, http://www.blackwell-synergy.com/doi/pdf/10.1111/j. 1467-8659.2007.01103.x

DOI: 10.1002/cav

Authors' biographies:

Dr L. H. You is currently a Senior Research Lecturer at the National Centre for Computer Animation, Bournemoth Media School, Bournemouth University, UK. His research interests are in computer graphics, computer animation and geometric modelling.

Xiaosong Yang is a research fellow in the National Centre for Computer Animation, Bournemouth Media School, Bournemouth University, UK. He received his bachelor's (1993) and master's degree (1996) in Computer Science from Zhejiang University, P.R. China, PhD (2000) in Computing Mechanics from Dalian University of Technology, P.R. China. He worked as PostDoc (2000–2002) in the Department of Computer Science and Technology of Tsinghua University for two years, and Research Assistant (2001–2002) at the 'Virtual Reality, Visualisation and Imaging Research Centre' of Chinese University of Hong Kong. His research interests include 3D modelling, animation, real-time rendering, virtual reality, virtual surgery simulation and computer-aided design.

Jian J. Zhang is Professor of Computer Graphics at the National Centre for Computer Animation and Director of Computer Animation Research Centre, Bournemouth Media School, Bournemouth University. His research interests include computer graphics, computer animation, physically based simulation, geometric modelling, medical simulation and visualisation.

DOI: 10.1002/cav